

AD-A159 457



TECHNICAL REPORT RE-CR-85-3

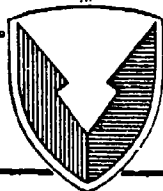
EXACT DETECTION PROBABILITY AND FLUCTUATION LOSS
FOR A PARTIALLY CORRELATED RAYLEIGH TARGET

Irving Kanter
ARO Contractor
277 Waltham Street
Lexington, MA 02173

JULY 1985

Prepared for:
Advanced Sensors Directorate
Research, Development, and Engineering Center

Contract No. DAAG29-81-C-0100



U.S. ARMY MISSILE COMMAND

Redstone Arsenal, Alabama 35898-5000

Approved for public release; distribution unlimited.

FILE COPY
0000

DTIC
ELECTE
OCT 1 1985
B

85 09_30 064

DISPOSITION INSTRUCTIONS

**DESTROY THIS REPORT WHEN IT IS NO LONGER NEEDED. DO NOT
RETURN IT TO THE ORIGINATOR.**

DISCLAIMER

**THE FINDINGS IN THIS REPORT ARE NOT TO BE CONSTRUED AS AN
OFFICIAL DEPARTMENT OF THE ARMY POSITION UNLESS SO DESIGNATED BY OTHER AUTHORIZED DOCUMENTS.**

TRADE NAMES

**USE OF TRADE NAMES OR MANUFACTURERS IN THIS REPORT DOES
NOT CONSTITUTE AN OFFICIAL INCREASEMENT OR APPROVAL OF
THE USE OF SUCH COMMERCIAL HARDWARE OR SOFTWARE.**

DELIVERY ORDER 0889

EXACT DETECTION PROBABILITY AND FLUCTUATION LOSS FOR A
PARTIALLY CORRELATED RAYLEIGH TARGET

IRVING KANTER

The views, opinions, and/or findings contained in this report are those of the author and should not be construed as an official Department of the Army position, policy, or decision, unless so designated by other documentation.

SECURITY CLASSIFICATION OF THIS PAGE (When Data Entered)

DD FORM 1 JAN 73 1473 EDITION OF 1 NOV 63 IS OBSOLETE

1 SECURITY CLASSIFICATION OF THIS PAGE (When Data Entered)

UNCLASSIFIED

SECURITY CLASSIFICATION OF THIS PAGE(When Data Entered)

tuation loss for a Gauss-Markov signal is determined as a function of number of pulses integrated, the correlation between pulses, and the specified detection and false alarm probabilities. This exact loss is compared to Barton's approximation.

ACKNOWLEDGEMENT

The author gratefully acknowledges the contributions of Dr. A.K. Newman who programmed the solution of the transcendental equation (58), calculated the P_D expressions (30), (66), (67) and generated Figures 1-7.

[illegible]

TABLE OF CONTENTS

	<u>Page</u>
PART ONE. EXACT DETECTION PROBABILITY	
I. INTRODUCTION.....	1
II. ANALYSIS.....	2
A. Marcum Model.....	4
B. Swerling Models.....	4
C. Partially Correlated Model.....	6
III. RESULTS.....	16
PART TWO. FLUCTUATION LOSS	
I. INTRODUCTION.....	25
II. BACKGROUND.....	26
III. ANALYSIS.....	29
REFERENCES.....	39

PART ONE. EXACT DETECTION PROBABILITY

I. INTRODUCTION

The determination of detection probability when the sum of N detected pulses of signal plus noise is compared to a threshold has been studied by Marcum, Swerling, Schwartz, and Vannicola, among others. Marcum¹ treated the non-fluctuating target; Swerling² treated two limiting fluctuating target situations (complete correlation and complete decorrelation) - he also presented a general method for treating arbitrary correlation³, but gave no results for particular correlation models; Schwartz⁴ achieved an exact solution when there are only two pulses; Vannicola⁵ has constructed a solution from Swerling's two extreme fluctuation models by considering M independent sets of N fully correlated pulses - his solution applies only to targets which are block correlated. This paper extends the previously referenced work and presents exact results for a Rayleigh target whose inphase (and quadrature) components have exponential correlation.

^{1,2,3,4,5} See References at end of text.

11. ANALYSIS

Denote the inphase and quadrature components of signal and noise respectively by the $N \times 1$ complex vectors $A+iB$ and $X+iY$. We assume (i) A, B are i.i.d.; (ii) X, Y are i.i.d. stationary Gaussian; (iii) the noise is additive and independent of the signal. Employing the Neyman-Pearson detection criterion, the probability of detection is given by

$$P_D \triangleq \int_{V_T}^{\infty} p_v(v) dv \quad (1)$$

where v is the integrator output normalized to the average per pulse noise power, i.e.,

$$v \triangleq \frac{|A+X|^2 + |B+Y|^2}{2\sigma^2} \quad (2)$$

and V_T is the normalized threshold determined by the specified probability of false alarm,

$$P_{FA} \triangleq \int_{V_T}^{\infty} p_v(v | |A|^2 + |B|^2 = 0) dv \quad (3)$$

In order to determine P_D we require the probability density function (pdf) of v . We first write $p_v(v)$ as an inverse Laplace transform

$$p_v(v) = \frac{1}{2\pi i} \int_{\gamma-i\infty}^{\gamma+i\infty} L_v(s) e^{sv} ds \quad (4)$$

Next recognizing

$$L_V(s) = \int_0^{\infty} p_V(v) e^{-sv} dv \quad (5)$$

as the expectation of e^{-sv} we proceed to calculate this expectation over the domain of A, B, X, Y i.e.,

$$L_V(s) = \int_{-\infty}^{\infty} \int_{-\infty}^{\infty} \int_{-\infty}^{\infty} p(A, B, X, Y) e^{-s \frac{|A+X|^2 + |B+Y|^2}{2\beta^2}} dA dB dX dY \quad (6)$$

In view of the three assumptions characterizing the signal and noise, the joint pdf of A, B, X, Y may be written as

$$p(A, B, X, Y) = p_A(A) p_B(B) \frac{1}{(2\pi\beta^2)^N} e^{-\frac{|X|^2 + |Y|^2}{2\beta^2}} \quad (7)$$

Thus (6) becomes

$$L_V(s) = \left[\int_{-\infty}^{\infty} p_A(A) dA \int_{-\infty}^{\infty} \frac{e^{-\frac{1}{2\beta^2} (s|A+X|^2 + |Y|^2)}}{(2\pi\beta^2)^{N/2}} dX \right]^2 \quad (8)$$

or, completing the square in X ,

$$L_V(s) = \left[\int_{-\infty}^{\infty} \frac{p_A(A) e^{-\frac{s}{s+1} \frac{|A|^2}{2\beta^2}}}{(s+1)^{N/2}} dA \int_{-\infty}^{\infty} \frac{e^{-\frac{s+1}{2\beta^2} |X + \frac{s}{s+1} A|^2}}{[2\pi\beta^2/(s+1)]^{N/2}} dX \right]^2 \quad (9)$$

Thus for any signal model we have the general formula

$$L_V(s) = \frac{1}{(s+1)^N} \left[\int_{-\infty}^{\infty} p_A(A) e^{-\frac{s}{s+1} \frac{|A|^2}{2\beta^2}} dA \right]^2 \quad (10)$$

A. Marcum Model

The non-fluctuating target may be accommodated by choosing

$$p_A(a_1, \dots, a_N) = \prod_{n=1}^N \delta(a_n - \alpha) \quad (11)$$

where $\delta(\cdot)$ is the Dirac delta function. Then (10) yields Marcum's result

$$L_V(s) = \frac{1}{(s+1)^N} e^{-\frac{s}{s+1} N\chi} \quad (12)$$

where χ is the per pulse ratio of signal power to average noise power, i.e.,

$$\chi \triangleq \frac{\alpha^2}{\beta^2} \quad (13)$$

B. Swerling Models

Typical radar targets are composed of a large number of scatterers whose distances relative to the radar change with body vibration and varying target aspect. The echoes from the individual scatters contribute

amplitude and phase terms which combine at the radar frequency to produce a fluctuating signal. Swerling has bounded the effects of target correlation by considering two limiting situations: The slow fluctuation model (unity amplitude correlation on a scan, scan-to-scan independence) and the fast fluctuation model (zero amplitude correlation on a scan, pulse-to-pulse independence). These may be accommodated by choosing respectively

$$p_A(a_1, \dots, a_N) = p_a(a_1) \prod_{n=2}^N \delta(a_n - a_1) \quad (14)$$

and

$$p_a(a_1, \dots, a_N) = \prod_{n=1}^N p_a(a_n) \quad (15)$$

Measurements⁶ of echoes from many types of radar targets confirm that the best characterization of the first order amplitude statistics is given by the Rayleigh distribution. (The best characterization of the autocorrelation function of the radar cross section is given by an exponential function.) Thus we assume

$$p_{\sqrt{a^2+b^2}}(r) = \frac{r}{\alpha^2} e^{-\frac{r^2}{2\alpha^2}} \quad (0 \leq r < \infty) \quad (16)$$

where $2\alpha^2$ is the average target cross section. In the remainder of this paper we confine our attention to this "Rayleigh target".

The inphase (or quadrature) components have first order statistics given by

$$p_a(a) = \frac{1}{\sqrt{2\pi} \alpha} e^{-\frac{a^2}{2\alpha^2}} \quad (17)$$

⁶See References at end of text.

Thus the general formula (10) specializes to Swerling's slow fluctuation result (case 1)

$$L_V(s) \Big|_{\rho=1} = \frac{1}{(s+1)^{N-1} [(1+N\chi)s+1]} \quad (18)$$

when (14) is employed as the correlation model and to Swerling's fast fluctuation result (case 2)

$$L_V(s) \Big|_{\rho=0} = \frac{1}{[(1+\chi)s+1]^N} \quad (19)$$

when (15) is employed as the correlation model.

C. Partially Correlated Model

In order to accommodate Rayleigh targets which give rise to partially correlated signals ($0 < \rho < 1$) we introduce the general correlation model

$$P_A(a_1, \dots, a_N) = \frac{e^{-\frac{1}{2\alpha^2} A^T C^{-1} A}}{(2\pi)^{N/2} |\alpha^2 C|^{1/2}} \quad (20)$$

where "T" denotes transpose and C is the covariance matrix of \mathbf{a} . For this correlated Rayleigh model, (10) yields

$$L_V(s) = \frac{1}{(s+1)^N} \left[\int_{-\infty}^{\infty} \frac{e^{-\frac{1}{2\alpha^2} A^T (C^{-1} + \frac{s}{s+1} \chi I) A}}{(2\pi)^{N/2} |\alpha^2 C|^{1/2}} dA \right]^2 \quad (21)$$

In (21) I is the identity matrix and χ [c.f. (13)] is the average signal-to-noise ratio. In order to evaluate the integral we assume that C is positive definite; then so also is C^{-1} ; hence when $s \geq 0$, $C^{-1} + \frac{s}{s+1} I$ is non-singular and (21) may be written as

$$L_V(s) = \frac{1}{(s+1)^N} \frac{1}{|C| |C^{-1} + \frac{s}{s+1} \chi I|} \left[\int_{-\infty}^{\infty} \frac{e^{-\frac{1}{2\alpha^2} A^T (C^{-1} + \frac{s}{s+1} \chi I) A}}{(2\pi)^{N/2} |\alpha^2 (C^{-1} + \frac{s}{s+1} \chi I)^{-1}|^{1/2}} dA \right]^2 \quad (22)$$

Since the integral equals unity we have

$$L_V(s) = \frac{1}{|(s+1)I + s\chi C|} \quad (23)$$

Expressing the determinant in terms of the (positive) eigenvalues $\lambda_1, \dots, \lambda_N$ of C the Laplace transform of $p_V(v)$ is given by

$$L_V(s) = \frac{1}{\prod_{n=1}^N [(1+\chi\lambda_n)s+1]} \quad (24)$$

Swerling's results may be obtained from this formula by choosing $\lambda_1 = N$, $\lambda_n = 0$ ($n \neq 1$) for the slow fluctuation case [c.f. (18)], and $\lambda_n \equiv 1$ for the fast fluctuation case [c.f. (19)]. These correspond respectively to the singular covariance matrix

$$C \Big|_{\rho=1} = \begin{bmatrix} N_0 & & 0 \\ & \ddots & \\ 0 & & 0 \end{bmatrix} \quad (25)$$

in which the first pulse contains all the average signal power of the pulse train and the remaining pulses contain no signal, and to the identity matrix

$$C \Big|_{\rho=0} = \begin{bmatrix} 1 & & 0 \\ & \ddots & \\ 0 & & 1 \end{bmatrix} \quad (26)$$

in which the total average signal power is uniformly distributed among the N pulses.

The inverse Laplace transform of (24) now yields the pdf of the integrator output. When $\chi=0$ we obtain

$$p_v(v|\chi=0) = e^{-v} \frac{v^{N-1}}{(N-1)!} \quad (27)$$

and when $\chi \neq 0$, (assuming distinct eigenvalues) we obtain

$$p_v(v) = \sum_{n=1}^N \prod_{\substack{k=1 \\ k \neq n}}^N \left[\left(1 - \frac{1+\chi\lambda_k}{1+\chi\lambda_n} \right) \right]^{-1} \frac{e^{-\frac{v}{1+\chi\lambda_n}}}{1+\chi\lambda_n} \quad (28)$$

Thus [c.f. (3)] the threshold, v_T , is given in terms of the specified P_{FA} by

$$P_{FA} = e^{-v_T} \sum_{n=0}^{N-1} \frac{v_T^n}{n!} \quad (29)$$

and [c.f. (1)] the probability of detection by

$$P_D = \sum_{n=1}^N \prod_{\substack{k=1 \\ k \neq n}}^N \left[\left(1 - \frac{1+\chi\lambda_k}{1+\chi\lambda_n} \right) \right]^{-1} e^{-\frac{v_T}{1+\chi\lambda_n}} \quad (30)$$

In order to calculate P_D for any particular correlation model we must provide a description of the correlation matrix. If the signal arises from a stationary process, then C is a symmetric Toeplitz matrix with N distinct elements. We should like to associate the eigenvalues with a single correlation parameter, ρ , in terms of which P_D may be conveniently characterized. For this purpose we assume that the signal is described by a first order Markov process. This is consistent with Edrington's measurements which show that the radar cross section is exponentially correlated.

Consider a signal which consists of a train of N pulses with uniform spacing T . Let the k, n element of C be taken as

$$C_{kn} = e^{-|k-n|Tv} \triangleq \rho^{|k-n|} \quad (0 < \rho < 1) \quad (31)$$

then

$$C = \begin{bmatrix} 1 & \rho & \cdots & \rho^{N-1} \\ \rho & 1 & \cdots & \rho^{N-2} \\ \vdots & \vdots & \ddots & \vdots \\ \rho^{N-1} & \rho^{N-2} & \cdots & 1 \end{bmatrix} \quad (32)$$

The eigenvalues of C provide a non-trivial solution to the matrix equation

$$[C - \lambda I]U = 0 \quad (33)$$

Since the sum of the eigenvalues equals the trace of C we have the relation

$$\sum_{n=1}^N \lambda_n = N \quad (34)$$

which we make use of later.

Consider first the special case of a low prf (pulse repetition frequency) waveform for which the interpulse spacing, T , is so large that the correlation of noncontiguous pulses may be neglected. Thus C becomes tri-diagonal and (33) is equivalent to a homogeneous bvp (boundary value problem). This consists of a set of homogeneous second order difference equations

$$\rho u_{n-1} + (1-\lambda)u_n + \rho u_{n+1} = 0 \quad (n=1, \dots, N) \quad (35)$$

together with the homogeneous boundary conditions

$$u_0 = u_{N+1} = 0 \quad (36)$$

Since the equation is linear and has constant coefficients, there are

two solutions in the form

$$u_n = \gamma^n \quad (37)$$

where

$$\gamma = \frac{\lambda-1}{2\rho} \pm \sqrt{\left(\frac{\lambda-1}{2\rho}\right)^2 - 1} \quad (38)$$

The condition $\left|\frac{\lambda-1}{2\rho}\right| \geq 1$ implies either $\lambda \geq 1+2\rho$ or $\lambda \leq 1-2\rho$, each of which

leads to a contradiction of (34). Hence we must have $\left|\frac{\lambda-1}{2\rho}\right| < 1$, i.e.,

$\gamma = e^{\pm i\theta}$ where

$$\cos \theta = \frac{\lambda-1}{2\rho} \quad (39)$$

We write the general solution to (35) in terms of $e^{\pm i n \theta}$ as

$$u_n = K_1 \cos n\theta + K_2 \sin n\theta \quad (40)$$

Since $u_0 = 0$, we have

$$u_n = K_2 \sin n\theta \quad (41)$$

and since $u_{N+1} = 0$, θ satisfies the transcendental equation

$$\sin (N+1)\theta = 0 \quad (42)$$

Further since (41) is a non-trivial solution, θ cannot equal 0 or π .

Thus the roots of (42) are

$$\theta_n = \frac{n}{N+1} \pi \quad (n=1, \dots, N) \quad (43)$$

Note that they are equally spaced in the open interval $(0, \pi)$. Equation (39) then yields the distinct eigenvalues

$$1-2\rho < \lambda_n = 1 + 2\rho \cos \theta_n < 1+2\rho \quad (n=1, \dots, N) \quad (44)$$

so that P_D is given by (30).

When the correlation of non-contiguous pulses may not be neglected we require the eigenvalues of the full C matrix. As is easily verified, the inverse matrix, C^{-1} , is the tri-diagonal matrix

$$C^{-1} = \frac{1}{1-\rho^2} \begin{bmatrix} 1 & -\rho & & & \\ -\rho & 1+\rho^2 & & & \\ & & \ddots & & \\ & & & 1+\rho^2 & -\rho \\ & & & -\rho & 1 \end{bmatrix} \quad (45)$$

Thus the eigenvalue problem to be solved is

$$(1-\rho^2) (C^{-1} - \frac{1}{\lambda} I) v = 0 \quad (46)$$

or

$$\begin{bmatrix} 1 - \frac{1-\rho^2}{\lambda} & -\rho & & & \\ -\rho & 1+\rho^2 - \frac{1-\rho^2}{\lambda} & & & \\ & & \ddots & & \\ & & & 1+\rho^2 - \frac{1-\rho^2}{\lambda} & -\rho \\ & & & -\rho & 1 - \frac{1-\rho^2}{\lambda} \end{bmatrix} \begin{bmatrix} v_1 \\ \vdots \\ v_N \end{bmatrix} = \begin{bmatrix} 0 \\ \vdots \\ 0 \end{bmatrix} \quad (47)$$

In the special case $N=2$, this becomes

$$\begin{bmatrix} 1 - \frac{1-\rho^2}{\lambda} & -\rho \\ -\rho & 1 - \frac{1-\rho^2}{\lambda} \end{bmatrix} \begin{bmatrix} v_1 \\ v_2 \end{bmatrix} = \begin{bmatrix} 0 \\ 0 \end{bmatrix} \quad (48)$$

which leads immediately to the distinct eigenvalues

$$\lambda = 1 \pm \rho \quad (49)$$

Equation (30) then yields P_D which may be written in the form

$$P_D = e^{-\frac{(1+\chi)V_T}{(1+\chi)^2 - (\rho\chi)^2}} \left[\frac{1+\chi}{\rho\chi} \sinh \frac{\rho\chi V_T}{(1+\chi)^2 - (\rho\chi)^2} + \cosh \frac{\rho\chi V_T}{(1+\chi)^2 - (\rho\chi)^2} \right] \quad (50)$$

which is the same result as that of Schwartz.

To solve (46) when $N>2$, we employ the technique developed for the low prf waveform; i.e., we again formulate and solve an equivalent homogeneous bvp. From (47) we have the equation

$$-\rho v_{n-1} + \left(1 + \rho^2 - \frac{1-\rho^2}{\lambda}\right) v_n - \rho v_{n+1} = 0 \quad (n=1, \dots, N) \quad (51)$$

and the boundary conditions

$$v_0 - \rho v_1 = 0 \quad (52)$$

$$v_{N+1} - \rho v_N = 0 \quad (53)$$

Again there is a solution of the form (37), provided that

$$\gamma = \left[1 + \rho^2 - \frac{1-\rho^2}{\lambda} \pm \sqrt{\left(1 + \rho^2 - \frac{1-\rho^2}{\lambda}\right)^2 - 4\rho^2} \right] / (2\rho) \quad (54)$$

Since $\left| \left(1 + \rho^2 - \frac{1 - \rho^2}{\lambda} \right) / (2\rho) \right| \geq 1$ implies either $\lambda \geq \frac{1 + \rho}{1 - \rho}$ or $\lambda \leq \frac{1 - \rho}{1 + \rho}$,

equation (34) cannot be satisfied. Thus we introduce the real angle θ by means of

$$\cos \theta \triangleq \frac{1 + \rho^2 - \frac{1 - \rho^2}{\lambda}}{2\rho} \quad (55)$$

and write the solution in the form (40). Application of the boundary conditions then yields the pair of equations

$$[1 - \rho \cos \theta] K_1 - [\rho \sin \theta] K_2 = 0 \quad (56)$$

$$[\cos (N+1)\theta - \rho \cos N\theta] K_1 + [\sin (N+1)\theta - \rho \sin N\theta] K_2 = 0 \quad (57)$$

whose determinant must vanish. Thus θ obeys the transcendental equation [c.f. (42)],

$$\sin(N+1)\theta - 2\rho \sin N\theta + \rho^2 \sin(N-1)\theta = 0 \quad (58)$$

Since the values $\theta=0, \pi$ do not permit a non-trivial solution to the bvp, the roots of (58) again lie in the open interval $(0, \pi)$. Since it has not been possible to solve (58) analytically, the following remarks allow a numerical solution to be easily achieved:

To show that there are exactly N roots between 0 and π we first write (58) as

$$[(1 + \rho^2) \cos \theta - 2\rho] \sin N\theta + [(1 - \rho^2) \sin \theta] \cos N\theta = 0 \quad (59)$$

then introduce the function $\phi(\theta)$ by means of

$$\sin \phi(\theta) \triangleq \frac{(1 - \rho^2) \sin \theta}{1 + \rho^2 - 2\rho \cos \theta} \quad (60)$$

$$\cos \phi(\theta) \triangleq \frac{(1+\rho^2)\cos\theta - 2\rho}{1 + \rho^2 - 2\rho \cos\theta} \quad (61)$$

so that (59) becomes

$$\sin [N\theta + \phi(\theta)] = 0 \quad (62)$$

[N.B. as $\rho \rightarrow 0$, $\phi(\theta) \rightarrow \theta$ and (62) \rightarrow (42)]

Since

$$\frac{d\phi}{d\theta} = \frac{1-\rho^2}{1+\rho^2 - 2\rho \cos\theta} > 0 \quad (63)$$

we have

$$\phi(\pi) = \phi(0) + \int_0^\pi \frac{1-\rho^2}{1+\rho^2 - 2\rho \cos\theta} d\theta = \pi \quad (64)$$

Since (62) represents a modulated sinusoid whose total phase increases monotonically from 0 at $\theta=0$ to $(N+1)\pi$ at $\theta=\pi$, it has exactly N distinct zero crossings in the open interval $(0, \pi)$.

Further, since $\frac{d^2\phi}{d\theta^2} < 0$ in $(0, \pi)$ and $\frac{d\phi}{d\theta} = 1$ at $\cos\theta=\rho$, the function

$\sin [N\theta + \phi(\theta)]$ oscillates more rapidly than does $\sin(N+1)\theta$ in the domain $0 < \theta < \cos^{-1}\rho$ and more slowly (but still more rapidly than does $\sin N\theta$) in the domain $\cos^{-1}\rho < \theta < \pi$. Using these observations concerning the spacing of the roots, it is an easy matter to accurately locate the roots by means of a Newton-Raphson method.

Denoting the roots by $\theta_1, \dots, \theta_N$ the eigenvalues [c.f. (55)] are given by

$$\frac{1-\rho}{1+\rho} < \lambda_n = \frac{1-\rho^2}{1+\rho^2 - 2\rho\cos\theta_n} < \frac{1+\rho}{1-\rho} \quad (n=1, \dots, N) \quad (65)$$

and the detection probability by (30).

Note that expansion of (65) into a power series in ρ yields a first order approximation which is identical to (44) - a useful check.

III. RESULTS

Figures 1-7 present detection probability versus per pulse average signal-to-noise ratio in dB for false alarm probability of 10^{-6} and $N=2, 4, 6, 10, 15, 20, 30$ pulses respectively.

The dashed curve is the Marcum result which was obtained by employing (11) in (10), performing the Laplace inversion and integrating the resulting pdf over the threshold; this leads to

$$P_D = P_{FA} + e^{-(V_T + N\chi)} \sum_{n=1}^{\infty} \frac{(N\chi)^n}{n!} \sum_{k=N}^{N-1+n} \frac{V_T^k}{k!} \quad (66)$$

The closest dark curve is the Swerling case 2 result ($\rho=0$) which was obtained by replacing V_T by $V_T/(1+\chi)$ in (29).

The next (lighter) curves are the results for $\rho=0.40, 0.60, 0.80, 0.90, 0.95, 0.99$ respectively.

The last (dark) curve is the Swerling case 1 result ($\rho=1$) which was obtained by performing the inverse Laplace transform of (18) and integrating the resulting pdf over the threshold; this leads to

$$P_D = P_{FA} + \frac{1}{1+N\chi} e^{-V_T} \sum_{n=1}^{\infty} \left(\frac{N\chi}{1+N\chi} \right)^n \sum_{k=N}^{N-1+n} \frac{V_T^k}{k!} \quad (67)$$

For $N=20$, the numerical instability exhibited at small values of χ when $\rho = 0.99$ is caused by the small eigenvalues [c.f. (65)] which cluster together; i.e., by indexing the eigenvalues according to size, it may be seen that the individual terms in (30) alternate in sign and increase in magnitude as the difference $\chi\lambda_n - \chi\lambda_k$ becomes smaller. This instability becomes more pronounced and occurs at even smaller values of ρ as N increases (it occurs at $\rho = 0.95$ when $N = 30$). In order to present a clean figure when $N = 30$, the curve for $\rho = 0.99$ has been deleted from figure 7.

The figures show that as ρ increases from zero to unity, more per pulse average signal-to-noise is required to achieve the same P_D . This increase, however, is smaller than one would intuitively expect; for example, increasing ρ from zero to one-half requires an additional increase of less than a dB in signal-to-noise at any $0.50 \leq P_D \leq 0.99$ and $N > 1$ while, for example at $P_D = 0.95$, increasing ρ from zero to one requires an increase of 5.2 dB for $N = 2$ or 10.6 dB for $N = 30$.

N - 2 PULSES, PFA - 10^{-6}
 NON-FLUCTUATING TARGET AND
 $\rho = 0, .4, .6, .8, .9, .95, .99, 1.0$

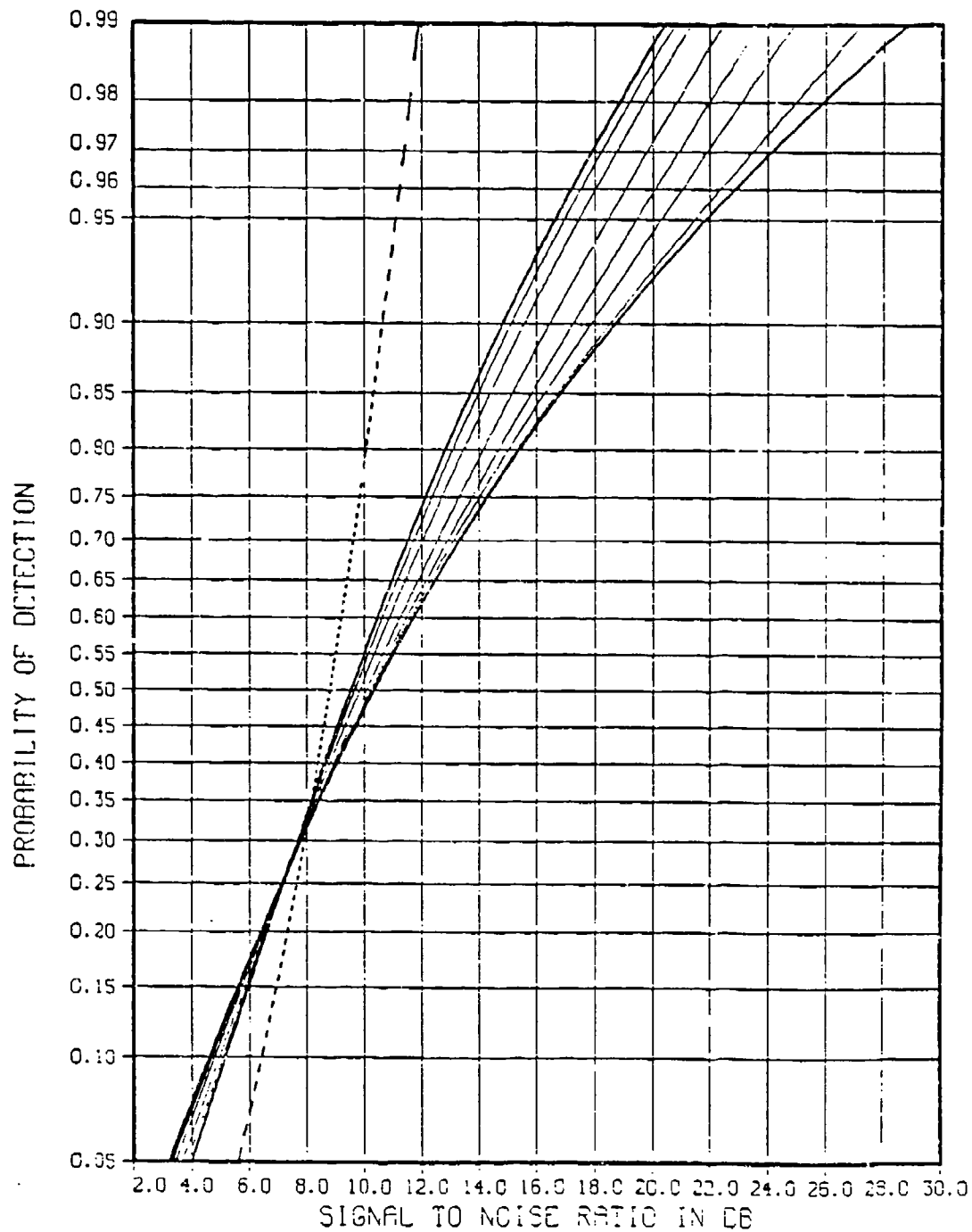


Figure 1.

N = 4 PULSES, PFA = 10^{-6}
 NON-FLUCTUATING TARGET AND
 $\rho = 0, .4, .6, .8, .9, .95, .99, 1.0$

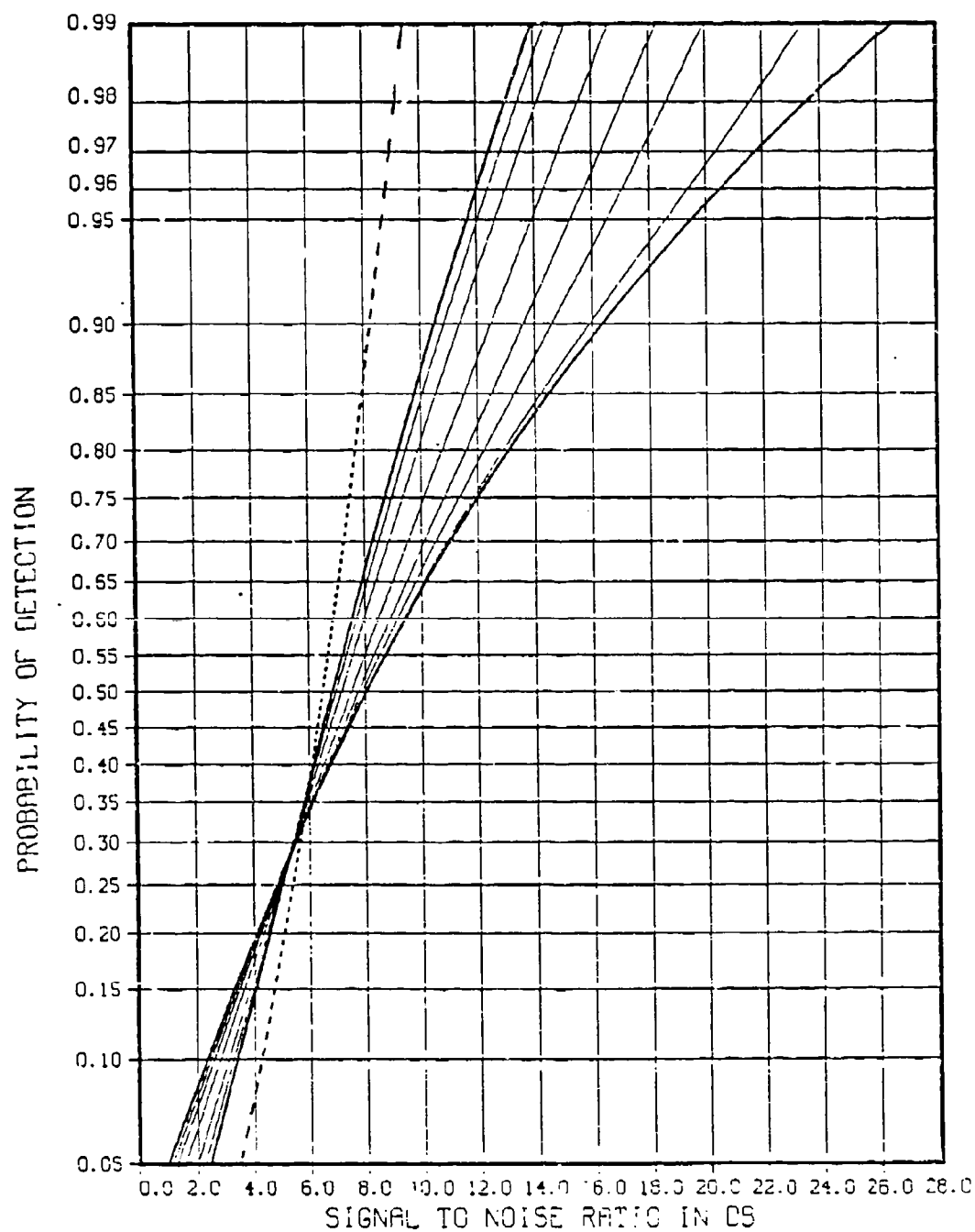


Figure 2.

$N = 6$ PULSES, $PFA = 10^{-6}$
 NON-FLUCTUATING TARGET AND
 $\rho = 0, .4, .6, .8, .9, .95, .99, 1.0$

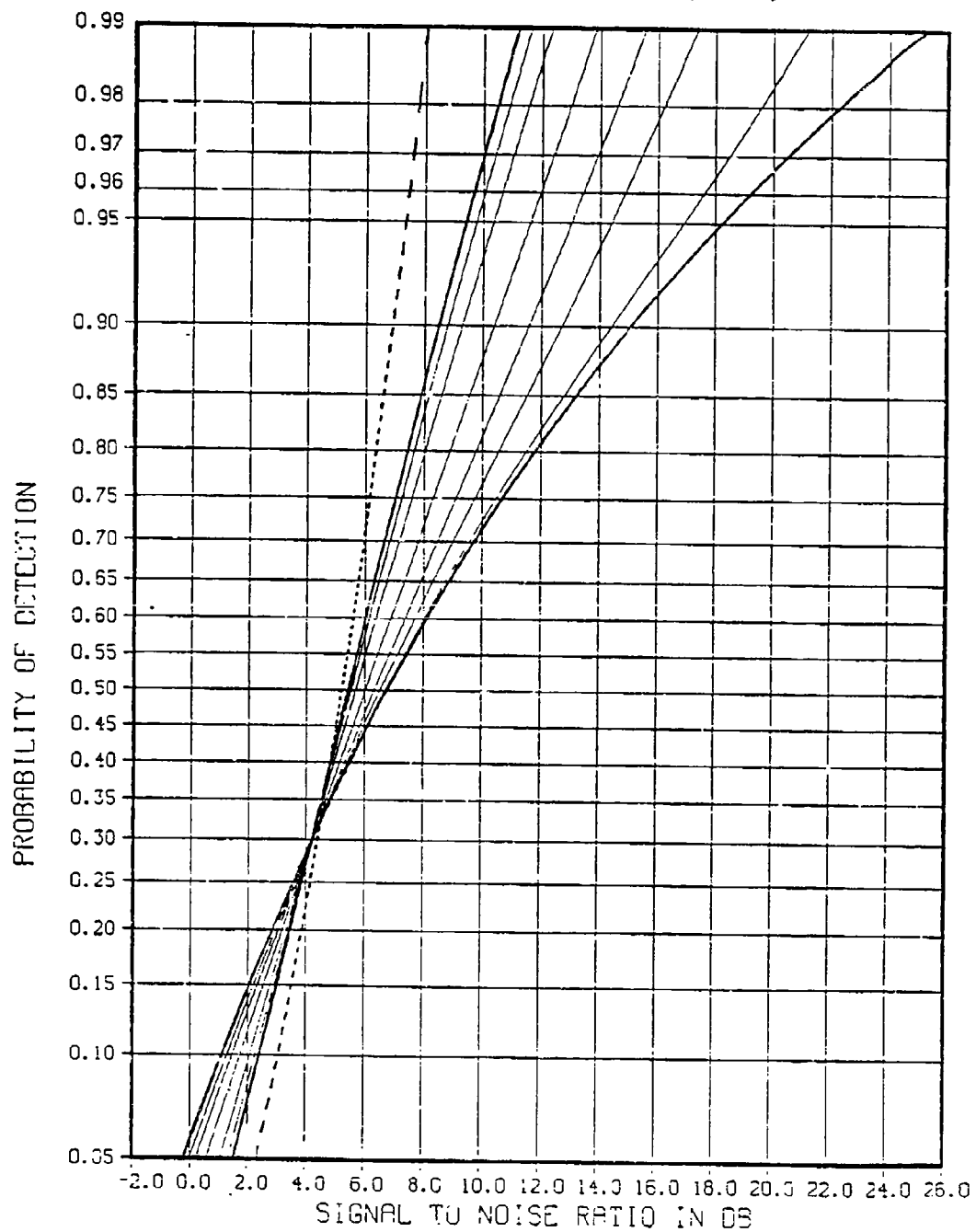


Figure 3.

$N = 10$ PULSES, $PFA = 10^{-6}$
 NON-FLUCTUATING TARGET AND
 $\rho = 0, .4, .6, .8, .9, .95, .99, 1.0$

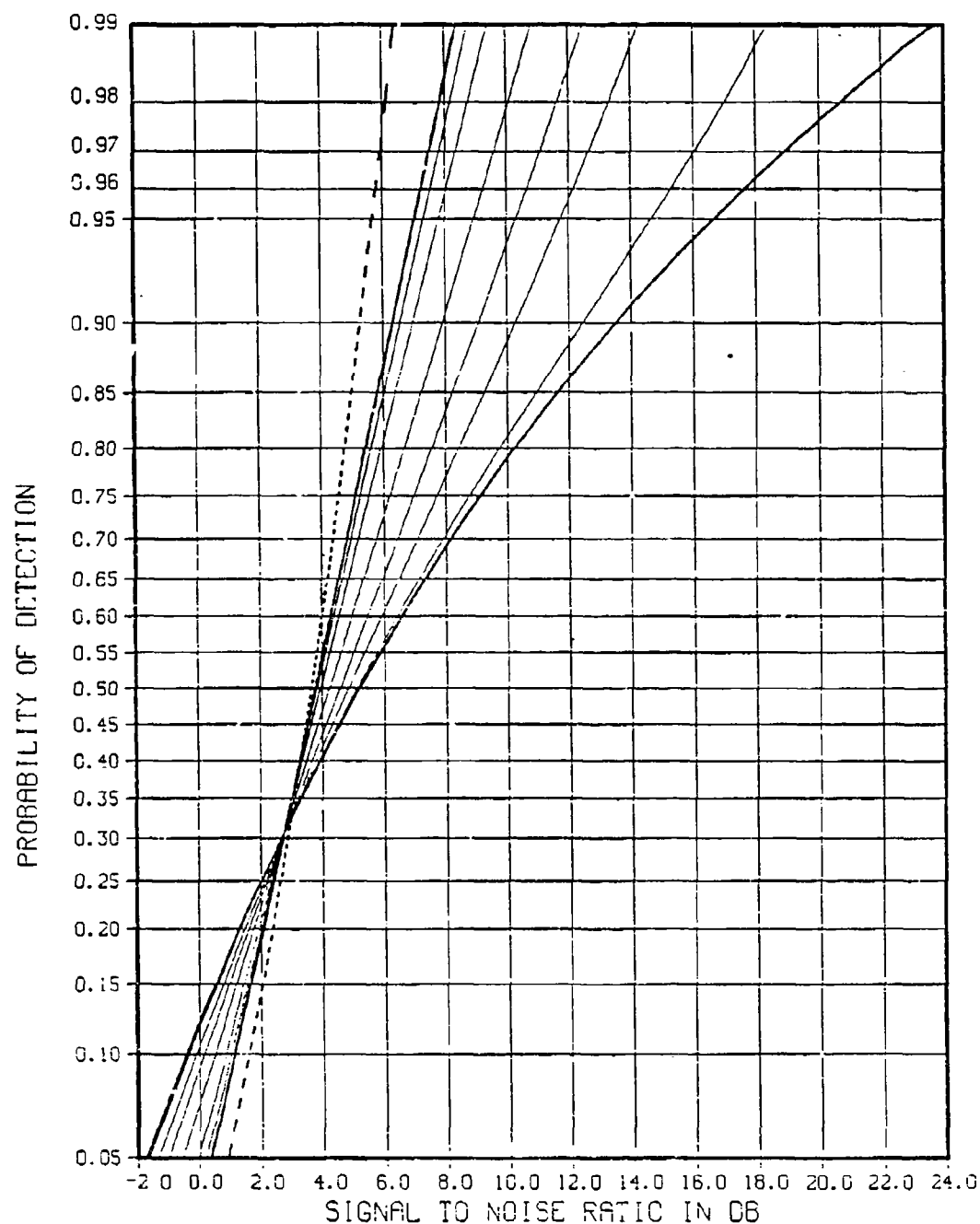


Figure 4.

N = 15 PULSES, PFA = 10^{-6}
 NON-FLUCTUATING TARGET AND
 $\rho = 0, .4, .6, .8, .9, .95, .99, 1.0$

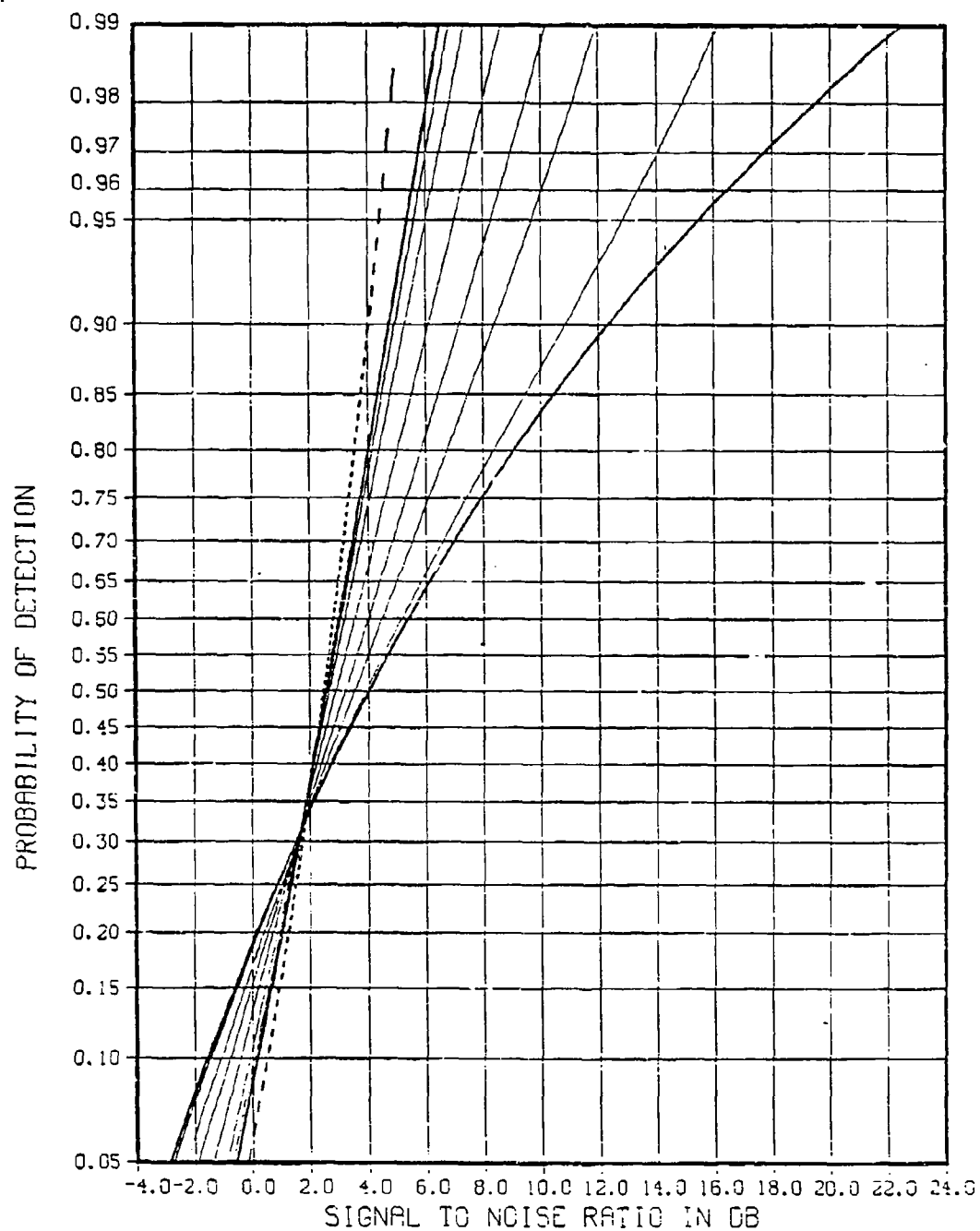


Figure 5.

N - 20 PULSES, PFA - 10^{-6}
NON-FLUCTUATING TARGET AND
RHC - 0, .4, .6, .8, .9, .95, .99, 1.0

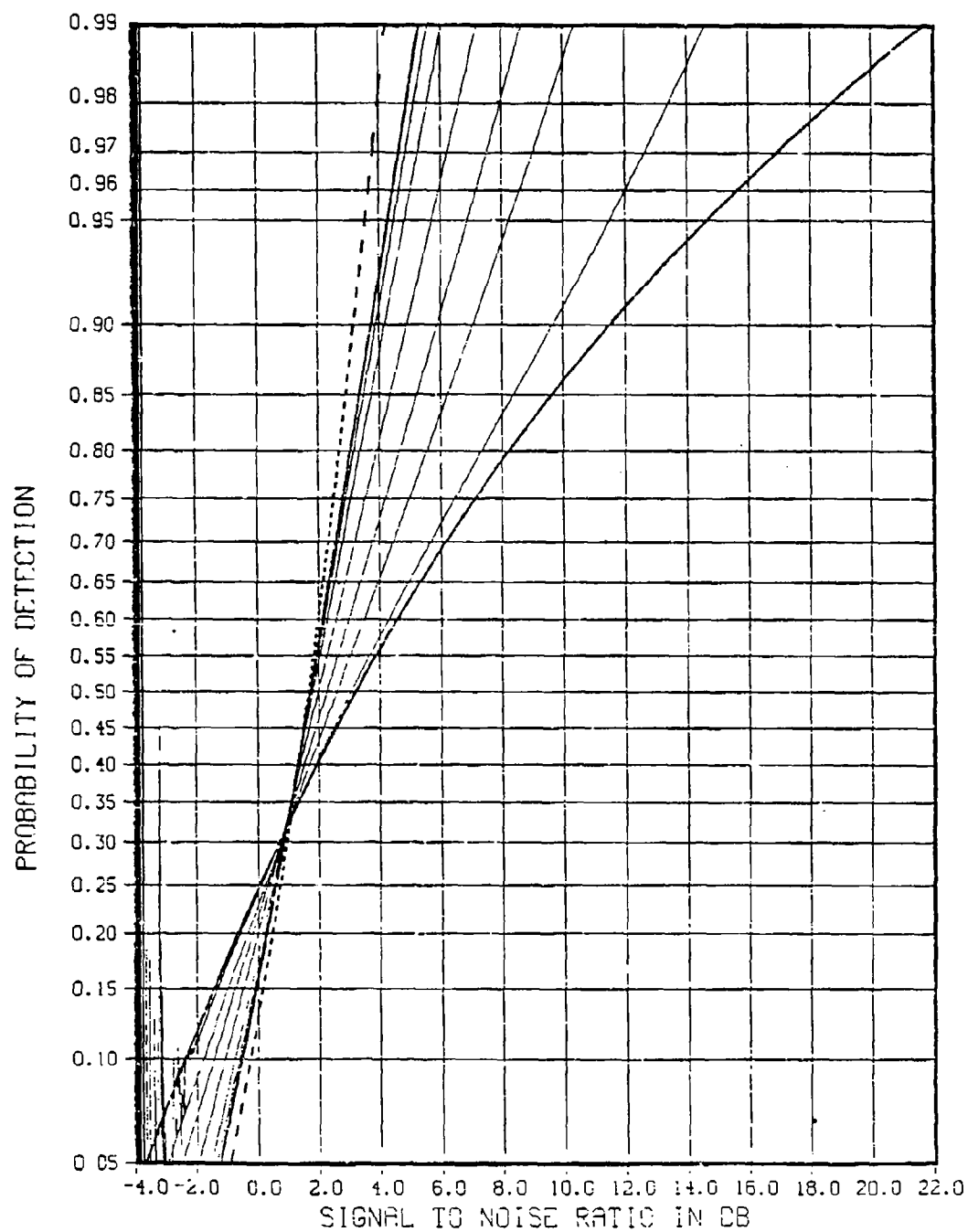


Figure 6.

N = 30 PULSES, PFA = 10^{-6}
 NON-FLUCTUATING TARGET AND
 $\rho = 0, .4, .6, .8, .9, .95, \text{ AND } 1.0$

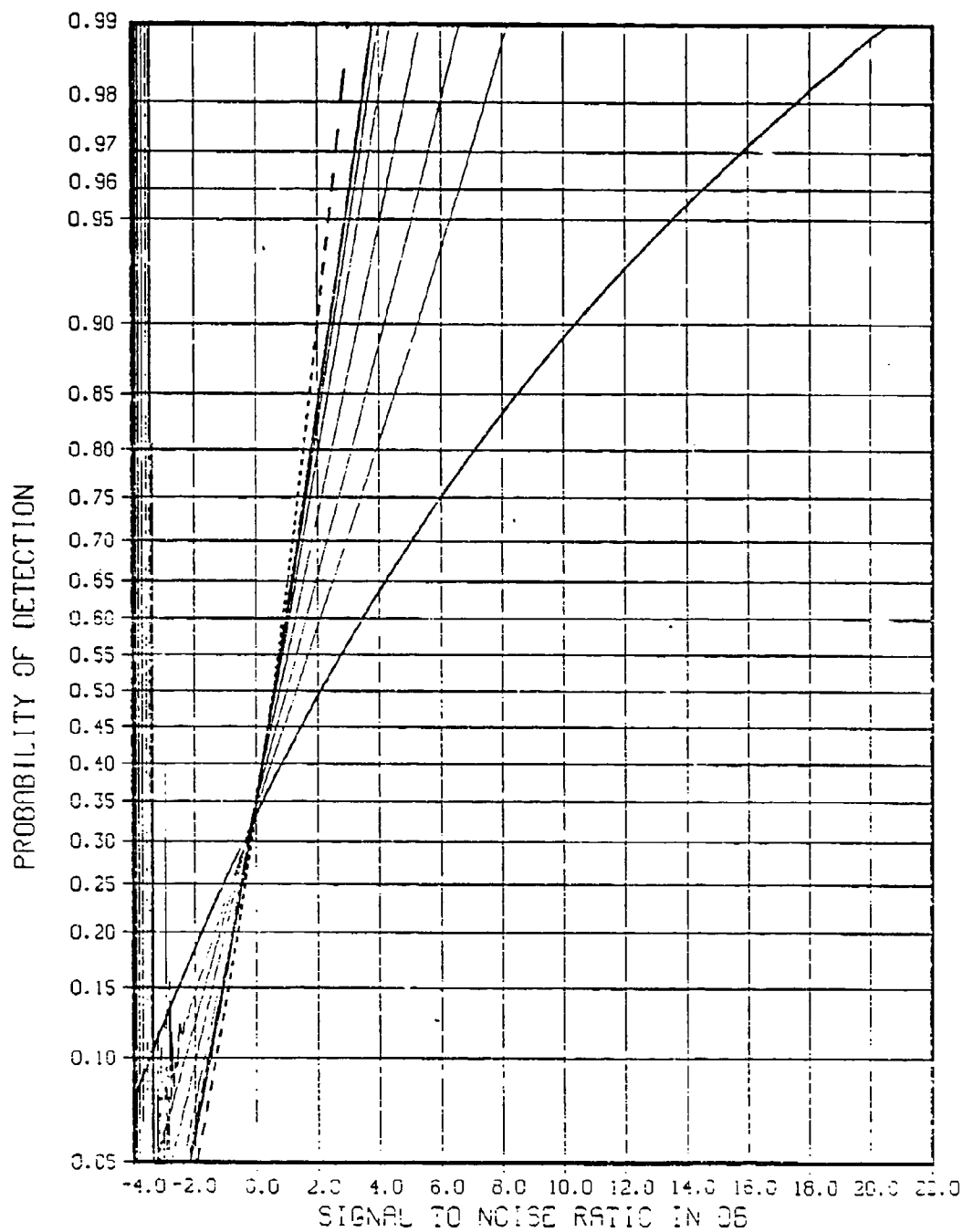


Figure 7.

PART TWO. FLUCTUATION LOSS

1. INTRODUCTION

The exact fluctuation loss for a Gauss-Markov signal is determined as a function of the number of integrated pulses, the correlation between contiguous pulses and the specified detection and false alarm probabilities. This exact loss is compared to Barton's⁷ approximation which calculates fluctuation loss by assuming a Swerling case 2 target and a reduced number of "independent" pulses. Two expressions for the number (N_e or N_I) of equivalent independent pulses are derived. The domain of validity of the approximations is established.

⁷See references at end of text.

11. BACKGROUND

Figures 1-7 of part 1 show that at fixed P_{FA} and N a greater per pulse average signal-to-noise ratio (detectability factor) is required to achieve a specified P_D (≥ 0.50) when the target fluctuates than when it does not. This required increase in detectability factor is called the fluctuation loss. For fixed P_D and P_{FA} it depends on the number of detected pulses and their correlation and will be denoted by $L_f(N, \rho)$.

Table I presents the detectability factors $D_0(N)$ for a non-fluctuating target, $D_2(N)$ for a Swerling case 2 ($\rho=0$) target and $D_1(N)$ for a Swerling case 1 ($\rho=1$) target at various P_D 's of interest; also shown is the normalized threshold voltage required to achieve the common P_{FA} of 10^{-6} . This table has been calculated from eqs. (66), (29) with V_T replaced by $V_T/(1+\chi)$, and (67) of part 1.

For the P_D 's of interest the fact that for $N > 1$,

$$L_f(N, 1) \triangleq D_1(N) - D_0(N) > D_2(N) - D_0(N) \triangleq L_f(N, 0)$$

is well known to radar systems engineers from the previously published work of Marcum and Swerling.

Whenever a surveillance radar encounters the situation $\rho \approx 1$, the target may lie in a deep fade for all N pulses received on a given scan, thus causing a detection to be missed. In order to avoid this situation some radar systems decorrelate the N signal returns by transmitting pulse-to-pulse frequency diverse waveforms. This certainly decreases the fluctuation loss from $L_f(N, \rho)$ to $L_f(N, 0)$ (a considerable reduction at high P_D and N) but involves increased system complexity and cost.

Fluctuation loss depends not only on P_{FA} and P_D but also on the fluctuation model and the correlation model. For $P_{FA} = 10^{-6}$, a Gaussian fluctuation model (Rayleigh envelope), and a first order Markov correlation model the analysis of part 1 yields the appropriate detectability factors for each N and ρ . By subtracting the detectability factor $D_0(N)$, we obtain the fluctuation losses, $L_f(N, \rho)$, of table II.

It is observed that the fluctuation loss increases monotonically with P_D and, except for the singular case $\rho = 1$, decreases monotonically with N . Of greater significance however is the nature of the monotonic increase in fluctuation loss with ρ and in particular its rate of increase as ρ approaches 1.

TABLE I
DETECTABILITY FACTORS AT $P_{FA} = 10^{-6}$

N	$P_D=0.50$	$P_D=0.70$	$P_D=0.90$	$P_D=0.95$	$P_D=0.99$	V_T (dB)
	D_0 (N)	D_0 (N)	D_0 (N)	D_0 (N)	D_0 (N)	
1	11.24	12.09	13.18	13.66	14.50	11.40
2	8.80	9.61	10.65	11.11	11.91	12.22
4	6.49	7.26	8.25	8.68	9.44	13.29
6	5.21	5.94	6.90	7.32	8.06	14.05
10	3.65	4.35	5.27	5.67	6.38	15.15
15	2.47	3.14	4.03	4.41	5.10	16.13
20	1.66	2.31	3.17	3.55	4.21	16.89
30	0.54	1.18	2.00	2.37	3.01	18.03
	D_2 (N)	D_2 (N)	D_2 (N)	D_2 (N)	D_2 (N)	
1	12.77	15.77	21.14	24.29	31.37	
2	9.52	11.53	14.83	16.62	20.47	
4	6.83	8.28	10.51	11.65	13.97	
6	5.4	6.65	8.49	9.41	11.22	
10	3.7	4.80	6.29	7.02	8.40	
15	2.54	3.46	4.75	5.36	6.52	
20	1.71	2.55	3.73	4.29	5.32	
30	0.58	1.34	2.39	2.88	3.78	
	D_1 (N)	D_1 (N)	D_1 (N)	D_1 (N)	D_1 (N)	
1	12.77	15.77	21.14	24.29	31.37	
2	10.33	13.32	18.69	21.84	28.91	
4	8.03	11.00	16.36	19.51	26.60	
6	6.74	9.71	15.07	18.21	25.30	
10	5.19	8.15	13.50	16.64	23.73	
15	4.00	6.96	12.31	15.45	22.54	
20	3.19	6.14	11.49	14.63	21.72	
30	2.08	5.03	10.37	13.51	20.57	

TABLE II
 $L_f(N, \rho)$ - FLUCTUATION LOSS (dB)

P_D	N	$\rho=0.00$	$\rho=0.40$	$\rho=0.60$	$\rho=0.80$	$\rho=0.90$	$\rho=0.95$	$\rho=0.99$	$\rho=1.0$
0.50	2	0.72	0.85	1.04	1.28	1.41	1.48	1.51	1.53
	4	0.34	0.46	0.65	1.00	1.26	1.40	1.49	1.54
	6	0.21	0.31	0.47	0.81	1.12	1.32	1.47	1.53
	10	0.12	0.19	0.29	0.58	0.92	1.19	1.43	1.54
	15	0.07	0.11	0.19	0.42	0.73	1.04	1.39	1.53
	20	0.05	0.08	0.14	0.32	0.60	0.93	1.34	1.53
	30	0.04	0.06	0.10	0.22	0.44	0.65	1.26	1.54
0.70	2	1.92	2.13	2.44	2.95	3.31	3.51	3.64	3.71
	4	1.02	1.24	1.58	2.26	2.86	3.22	3.57	3.74
	6	0.71	0.90	1.21	1.86	2.54	3.06	3.53	3.77
	10	0.45	0.59	0.83	1.40	2.08	2.72	3.44	3.80
	15	0.32	0.42	0.61	1.08	1.71	2.35	3.35	3.82
	20	0.24	0.33	0.48	0.88	1.45	2.12	3.23	3.83
	30	0.16	0.22	0.33	0.64	1.12	1.74	3.04	3.85
0.90	2	4.18	4.49	4.93	5.79	6.59	7.21	7.88	8.04
	4	2.26	2.59	3.13	4.23	5.36	6.36	7.73	8.11
	6	1.59	1.90	2.39	3.48	4.66	5.79	7.65	8.17
	10	1.02	1.27	1.68	2.65	3.78	5.00	7.44	8.23
	15	0.72	0.91	1.25	2.11	3.15	4.33	7.24	8.28
	20	0.56	0.72	1.01	1.73	2.72	3.87	6.98	8.32
	30	0.39	0.52	0.73	1.32	2.17	3.23	6.58	8.37
0.95	2	5.51	5.84	6.33	7.33	8.32	9.18	10.52	10.73
	4	2.97	3.36	3.96	5.24	6.60	7.86	10.32	10.83
	6	2.09	2.44	3.03	4.28	5.68	7.08	10.22	10.89
	10	1.35	1.64	2.13	3.27	4.62	6.06	9.93	10.97
	15	0.95	1.19	1.60	2.58	3.84	5.26	9.66	11.04
	20	0.74	0.94	1.29	2.16	3.33	4.69	9.32	11.08
	30	0.51	0.67	0.94	1.65	2.66	3.92	8.79	11.14
0.99	2	8.56	8.91	9.47	10.61	11.83	13.04	16.70	17.00
	4	4.53	4.98	5.70	7.22	8.88	10.56	16.38	17.16
	6	3.16	3.60	4.32	5.84	7.56	9.34	16.22	17.24
	10	2.02	2.40	3.02	4.44	6.13	7.93	15.77	17.35
	15	1.42	1.74	2.27	3.52	5.11	6.87	15.34	17.44
	20	1.11	1.38	1.86	3.02	4.46	6.16	14.80	17.51
	30	0.77	0.99	1.38	2.31	3.61	5.10	13.94	17.56

For example, suppose all we know concerning the target returns is that they are not independent; if we make the usual assumption that they are fully correlated (i.e., $\rho=1$) and integrate 30 pulses to achieve required P_D 's of say 0.90, 0.95, 0.99 respectively, then a system which employs pulse-to-pulse frequency diversity could recover the fluctuation losses [$L_f(30,1) - L_f(30,0)$] of respectively, 8.0, 10.6, and 17.8 dB. If however ρ is not in fact equal to 1.0 but is instead 0.9 then the recoverable fluctuation losses are only 1.8, 2.2, 2.8 dB respectively (at $\rho=0.8$ the recoverable losses are even smaller, viz., 0.9, 1.1 and 1.5 dB). Thus the trade-off of system complexity versus recoverable fluctuation loss is markedly affected by knowledge of the dependence of fluctuation loss on signal correlation - a dependence established in part I of this paper.

In summary, the usually employed assumption, $\rho=1$, should not be facilely invoked simply because the signal returns are known to lack total independence. Doing so results in an extremely optimistic estimate of the benefits which can be achieved by employing frequency diversity.

III. ANALYSIS

e next consider two approximations which greatly simplify the determination of fluctuation loss for any correlation model. Barton⁷ introduces the concept of the number of equivalent "independent" pulses; this is defined by

$$N_e \triangleq \text{Min.} \left[N, 1 + \frac{t_o}{t_c} \right] \quad (67)$$

In (67) t_o is the observation time and t_c is the correlation time (which Barton defines for any correlation model as the reciprocal of the effective noise bandwidth of the two sided fluctuation spectrum). The definition, (67) is assumed to be valid independent of P_D or P_{FA} . Barton's two conjectures state;

$$L_f(N, \rho) \approx L_f(N_e, 0) \quad (\text{FIRST CONJECTURE}) \quad (68)$$

$$L_f(N_e, 0) \approx \frac{1}{N_e} L_f(1, \rho) \quad (\text{SECOND CONJECTURE}) \quad (69)$$

The validity of these conjectures will now be tested against the exact results available from our analysis of the first order Markov correlation model. We begin by calculating Barton's N_e .

In (67) we interpret t_c as the correlation time of the process at the detec-

⁷ See references at end of text.

tor output. Thus letting x and y denote i.i.d. stationary Gaussians which represent the inphase and quadrature components of signal at the detector input, the detector output becomes

$$z(t) \triangleq x^2(t) + y^2(t) \quad (70)$$

Its average (denoted by an overbar) is

$$\bar{z}(t) = \overline{x^2(t)} + \overline{y^2(t)} = 2R_x(0) \quad (71)$$

where [c.f. (31)]

$$R_x(\tau) = R_x(0) e^{-\nu|\tau|} \quad (72)$$

is the autocorrelation of the inphase (or quadrature) Markov process.

The covariance function at the detector output is

$$R_{z-z}(\tau) = \overline{[z(t) - \bar{z}(t)][z(t+\tau) - \bar{z}(t+\tau)]} = 2[R_x^2(\tau) - R_x^2(0)] \quad (73)$$

which, since $x(t)$ is a Gaussian process, yields

$$R_{z-z}(\tau) = 4R_x^2(\tau) \quad (74)$$

The "two sided fluctuation spectrum" is interpreted as the Fourier transform of the covariance function, i.e.,

$$S_x(f) = \int_{-\infty}^{\infty} 4R_x^2(0) e^{-2\nu|\tau|} e^{-i2\pi f\tau} d\tau = 4R_x^2(0) \frac{4\nu}{4\nu^2 + (2\pi f)^2} \quad (75)$$

This has an effective noise bandwidth, f_B , given by

$$f_B \triangleq \frac{\int_{-\infty}^{\infty} S_x(f) df}{S_x(0)} = \frac{R_{z-z}(0)}{S_x(0)} = \nu \quad (76)$$

Since the observation time is $(N-1)T$ and [c.f. (31)] $\rho = e^{-\nu T}$ the correlation time t_c , is $T/\ln \frac{1}{\rho}$. Thus

$$N_e(N, \rho) = \text{Min. } [N, 1 + (N-1) \ln \frac{1}{\rho}] \quad (77)$$

A more common definition of the number of independent integrated pulses is the increase in the ratio of squared mean to variance when N pulses are summed, i.e., define

$$V_N \triangleq \sum_{n=1}^N (x_n^2 + y_n^2) \quad (78)$$

then

$$N_I \triangleq \frac{\bar{V}_N^2 / \sigma_{V_N}^2}{\bar{V}_1^2 / \sigma_{V_1}^2} \quad (79)$$

It is easily shown that

$$N_I = N^2 \frac{\sigma_{V_1}^2}{\bar{V}_N^2} = \frac{N^2}{N + 2 \sum_{m=1}^{N-1} (N-m) R_x^2(m) / R_x^2(0)} \quad (80)$$

Since for the first order Markov model

$$R_x(m) = R_x(0) \rho^{|m|} \quad (81)$$

eq. (80) yields

$$N_I(N, \rho) = \frac{N}{1 + \frac{2\rho^2}{1-\rho^2} \left(1 - \frac{1}{N} \frac{1-\rho^{2N}}{1-\rho^2} \right)} \quad (82)$$

Note that $N_e \geq N_I$ except at $N = 1$ or $\rho = 1$, or $\rho = 0$ where equality obtains. Table III compares N_e with N_I for the N and ρ of table II.

Figures 8-12 are plots of the exact fluctuation losses of table II versus N_e .

the number of equivalent independent pulses as defined by Barton. The solid curves represent $L_f(N_e, 0)$, i.e., the left side of (69). Aside from a negligible positive curvature which is most pronounced at low N_e and high P_D , these do (as Barton conjectures) exhibit a linear decrease with N_e . The dashed curves represent the right side of (69), i.e., $\frac{1}{N_e} L_f(1, \rho)$. We see that the solid and

dashed curves are within 1/2 dB of each other; further we note that

$$L_f(N_e, 0) < \frac{1}{N_e} L_f(1, \rho) \quad (P_D = 0.50) \quad (83)$$

$$L_f(N_e, 0) > \frac{1}{N_e} L_f(1, \rho) \quad (P_D = 0.70, 0.90, 0.95, 0.99) \quad (84)$$

In Figures 10-12 the upper solid curve is the continuation of $L_f(N_e, 0)$ into the region $10 \leq N_e \leq 30$ (divide the ordinate by 10 and multiply the abscissa by 10). The dashed curve, $\frac{1}{N_e} L_f(1, \rho)$, is its own continuation.

The symbols \cdot , \times , \circ , Δ , \square , ∇ , identify values of $L_f(N, \rho)$ for $\rho = 0.40, 0.60, 0.80, 0.90, 0.95, 0.99$ respectively.

We see that for $P_D = 0.50$ and 0.70 , Barton's first conjecture underestimates the exact fluctuation loss by a fraction of a dB. For $P_D = 0.90, 0.95, 0.99$ the first conjecture overestimates the exact fluctuation loss at small N_e (by more than a dB at $P_D = 0.95$ and by several dB at $P_D = 0.99$) and underestimates the exact fluctuation loss by less than a dB at large N_e . Since the fluctuation loss monotonically decreases with N_e , Barton's first conjecture gives a result which is conservative when the losses are large, and optimistic when the losses are small.

If one were to use N_I instead of N_e to represent the number of independent pulses, the symbols representing $L_f(N, \rho)$ would shift to the left so that the approximations would become even more conservative at $P_D = 0.90, 0.95, 0.99$ when the losses are large. Thus Barton's N_e is the preferred approximation for $P_D \geq 0.90$ (large losses), while the approximation using N_I is to be preferred for $P_D \leq 0.70$ (small losses).

TABLE III

EQUIVALENT NUMBER OF INDEPENDENT PULSES

ρ	N=2		N=4		N=6		N=10		N=15		N=20		N=30	
	N_e	N_I	N_e	N_I	N_e	N_I	N_e	N_I	N_e	N_I	N_e	N_I	N_e	N_I
0.40	1.92	1.72	3.75	3.16	5.58	4.60	9.25	7.49	13.83	11.11	18.41	14.72	27.57	21.96
0.60	1.51	1.47	2.53	2.36	3.55	3.27	5.60	5.13	8.15	7.47	10.71	9.82	15.81	14.52
0.80	1.22	1.22	1.67	1.60	2.12	1.99	3.01	2.79	4.12	3.85	5.24	4.92	7.47	7.10
0.90	1.10	1.10	1.32	1.28	1.53	1.44	1.95	1.79	2.48	2.25	3.00	2.73	4.06	3.73
0.95	1.05	1.05	1.15	1.13	1.26	1.21	1.46	1.36	1.72	1.57	1.97	1.78	2.49	2.23
0.99	1.01	1.01	1.03	1.03	1.05	1.04	1.09	1.07	1.14	1.10	1.19	1.14	1.29	1.21

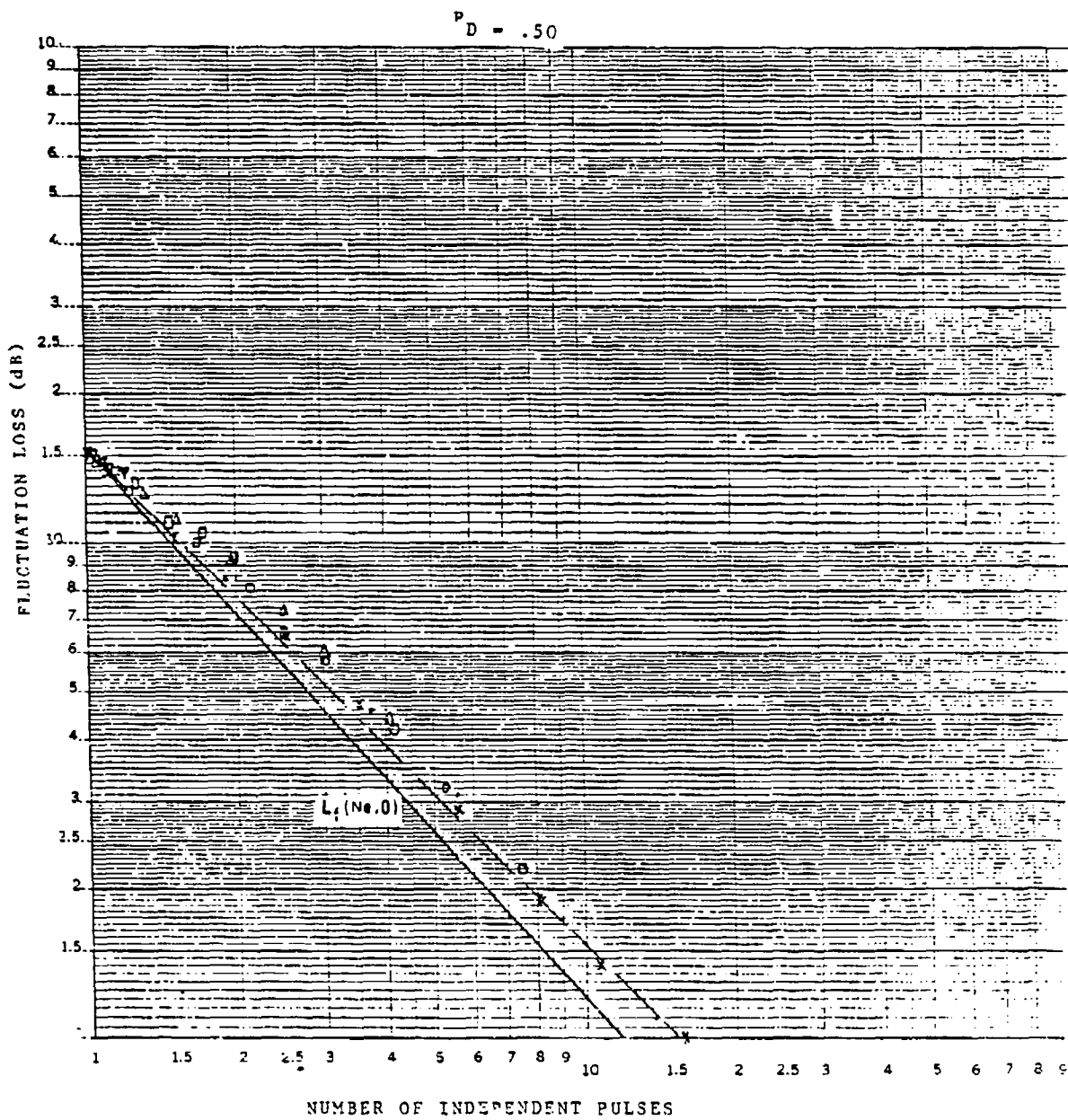


Figure 8.

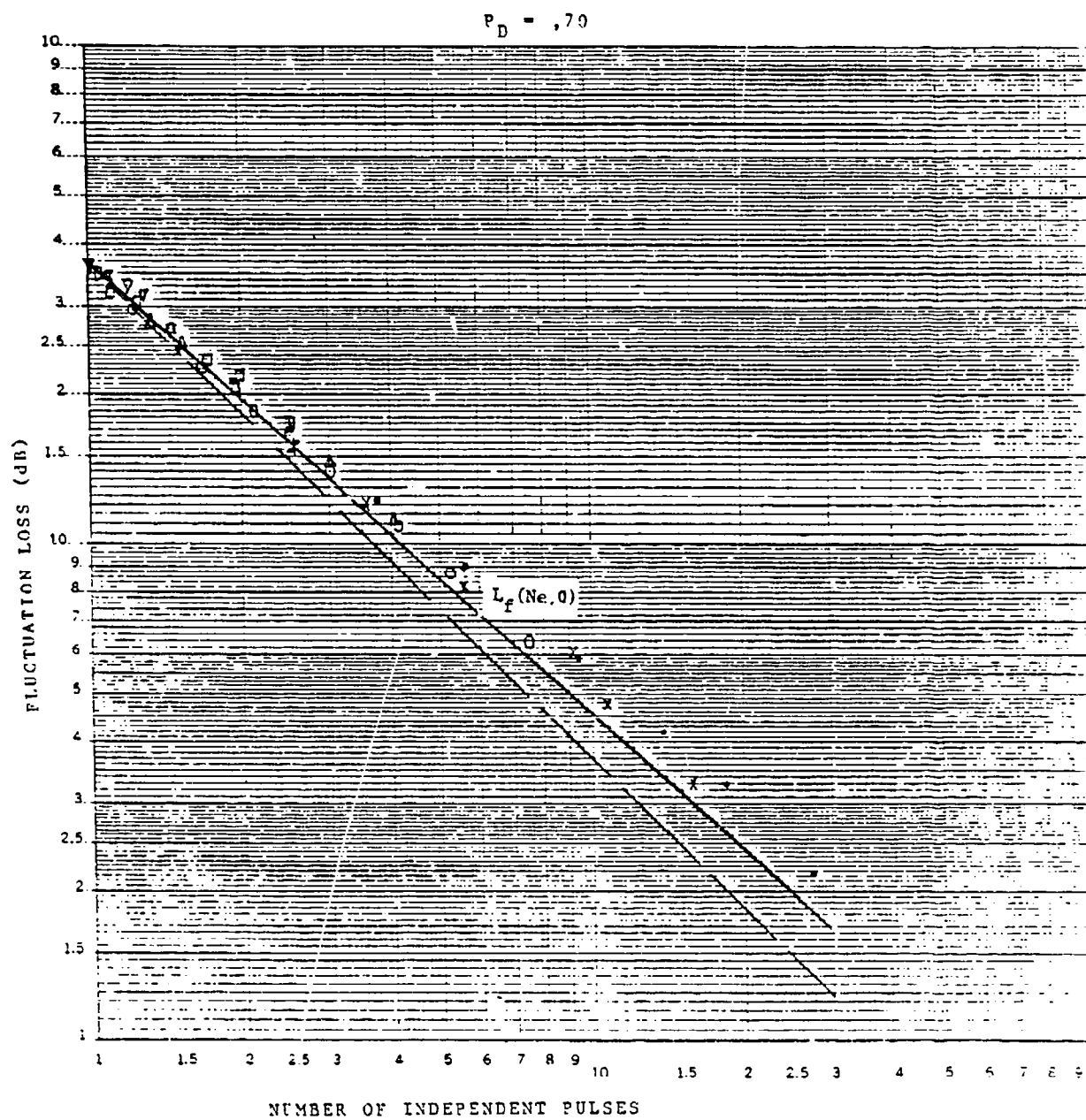


Figure 9.

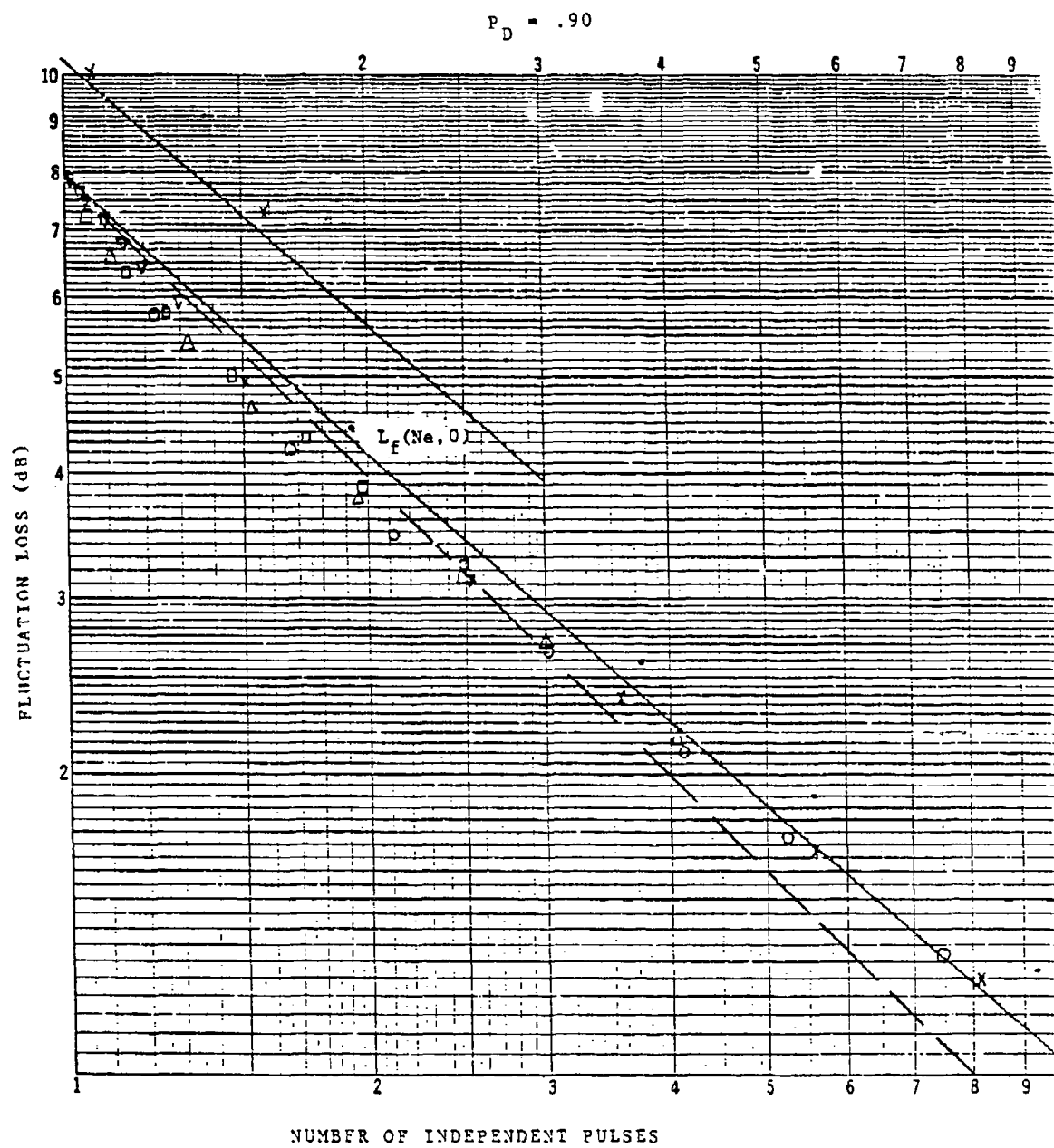
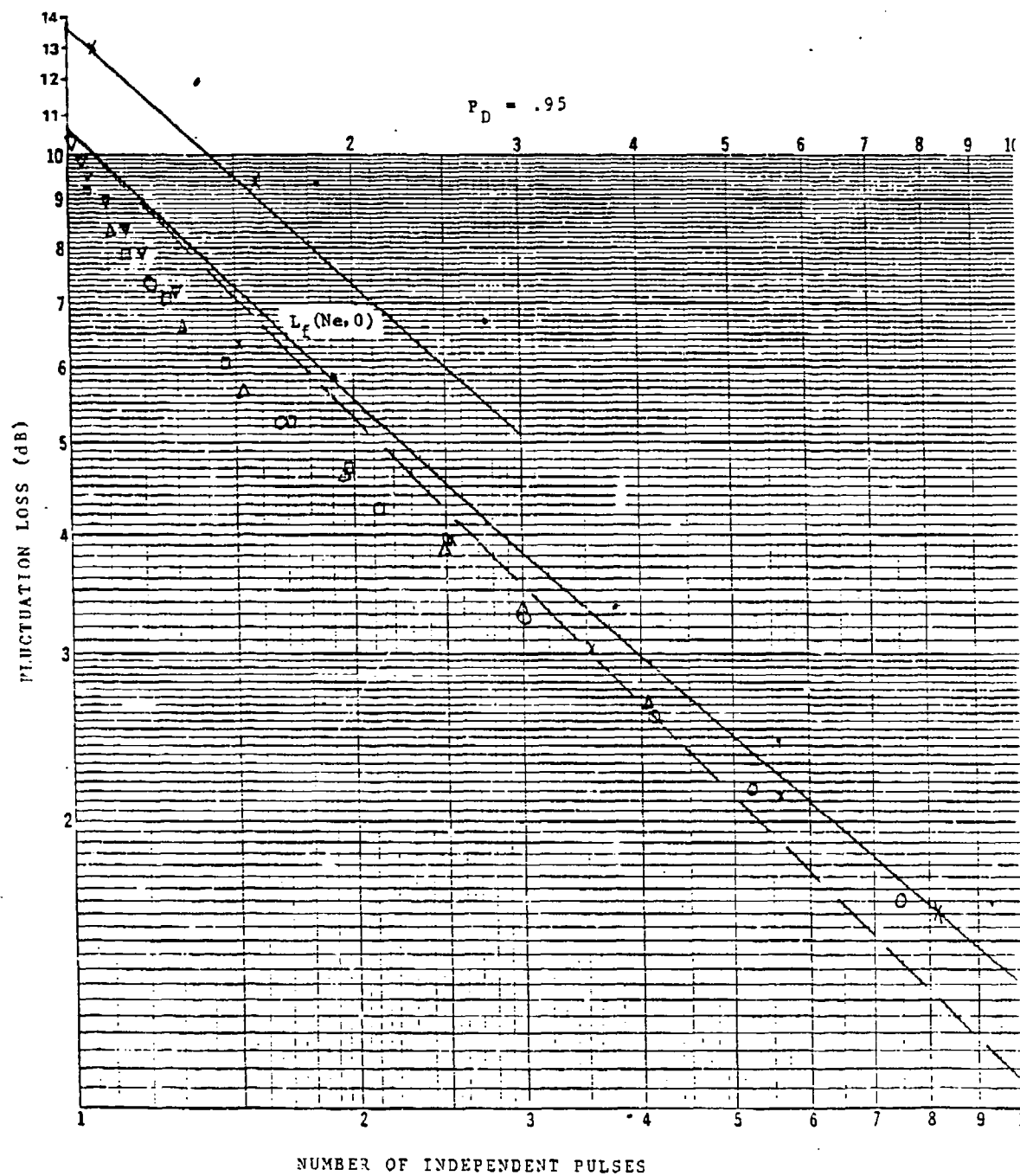


Figure 10.



$$P_D = .99$$

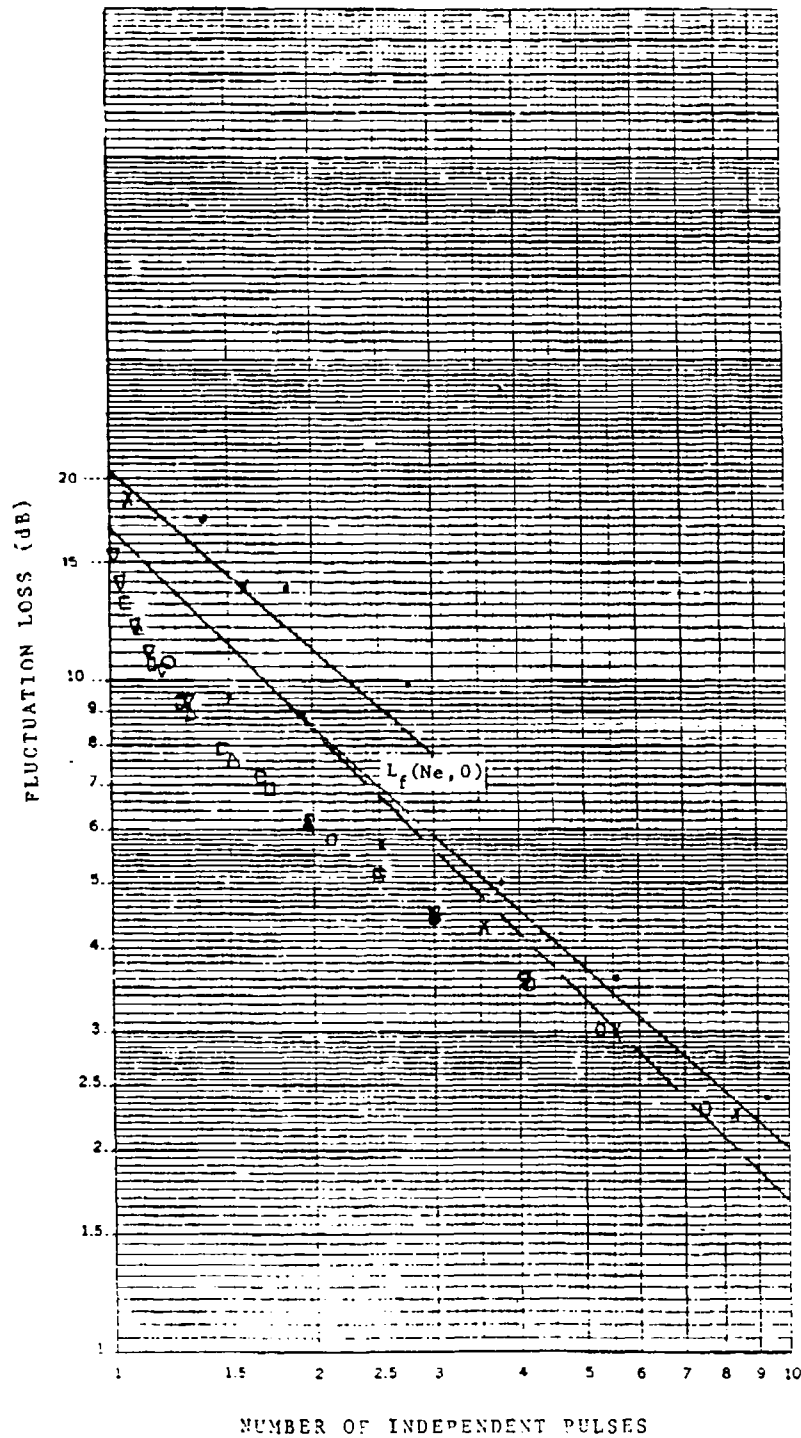


Figure 12.

REFERENCES

- 1) J.I. Marcum, "A Statistical Theory of Target Detection by Pulsed Radar, " IRE Trans. Information Theory, Vol. IT.-6 pp. 59-145, April 1960.
- 2) P. Swerling, "Probability of Detection of Fluctuating Targets," IRE Trans. Information Theory, Vol. IT.-6 pp. 269-308, April 1960.
- 3) P. Swerling, "Detection of Pulsed Signals in the Presence of Noise," IRE Trans. Information Theory, Vol. IT.-3 pp. 175-178, September 1957.
- 4) M. Schwartz, "Effects of Signal Fluctuations in the Detection of Pulsed Signals in Noise," IRE Trans. Information Theory, Vol. IT.-2 pp. 66-71, June 1956.
- 5) V. Vannicola, "Detection of Slow Fluctuating Targets with Frequency Diverse Channels," Trans. Aerospace and Electronic Systems, Vol. AES-10, January 1974.
- 6) T.S. Edrington, "The Amplitude Statistics of Aircraft Radar Echoes," IEEE Transactions on Military Electronics, Vol. MIL-9, No. 1, Jan. 1965
- 7) D.K. Barton, "Simple Procedure for Radar Detection Calculations," IEEE Trans. Aerospace and Electronic Systems, Vol. AES-5, September 1969.

DISTRIBUTION

	<u>Copies</u>
US Army Materiel System Analysis Activity	
ATTN: AMXSY-MP	1
Aberdeen Proving Ground, MD 21005	
ITT Research Institute	
ATTN: GACIAC	1
10 West 35th Street	
Chicago, IL 60616	
AMSMI-R, Dr. McCorkle	1
Dr. Rhoades	1
-RE, Mr. Pittman	1
-RE	1
-REL	1
-REG	1
-REM	1
-RER	15
-RPR, Reference	1
-RPT, Record Copy	1
-LP, Mr. Voigt	